

Supplementary Materials for

Ancient genome-wide analyses infer kinship structure in an Early Medieval Alemannic graveyard

Niall O'Sullivan*, Cosimo Posth, Valentina Coia, Verena J. Schuenemann, T. Douglas Price, Joachim Wahl, Ron Pinhasi, Albert Zink*, Johannes Krause*, Frank Maixner*

*Corresponding author. Email: niall.o-sullivan@ucdconnect.ie (N.O.); krause@shh.mpg.de (J.K.); albert.zink@eurac.edu (A.Z.); frank.maixner@eurac.edu (F.M.)

Published 5 September 2018, *Sci. Adv.* 4, eaao1262 (2018)

DOI: 10.1126/sciadv.aao1262

The PDF file includes:

Supplementary Materials and methods

Fig. S1. Photographs of burial goods with most specific cultural identifying markers.

Fig. S2. Isotope $^{86}\text{Sr}/^{87}\text{Sr}$ and $\delta^{18}\text{O}$ values for enamel from teeth.

Fig. S3. Overlaying shotgun and mtDNA deamination plots from mapDamage quantification against the reference genome.

Fig. S4. Genetic sex estimates from genome-wide capture.

Fig. S5. Admixture estimates for west Eurasians, Niederstotzingen, and selected ancient individuals.

Fig. S6. F3 outgroup statistics for Niederstotzingen 1 using Mbuti as an outgroup.

Fig. S7. F3 outgroup statistics for Niederstotzingen 3A using Mbuti as an outgroup.

Fig. S8. F3 outgroup statistics for Niederstotzingen 3B using Mbuti as an outgroup.

Fig. S9. F3 outgroup statistics for Niederstotzingen 3C using Mbuti as an outgroup.

Fig. S10. F3 outgroup statistics for Niederstotzingen 6 using Mbuti as an outgroup.

Fig. S11. F3 outgroup statistics for Niederstotzingen 9 using Mbuti as an outgroup.

Fig. S12. F3 outgroup statistics for Niederstotzingen 12B using Mbuti as an outgroup.

Fig. S13. F3 outgroup statistics for Niederstotzingen 12C using Mbuti as an outgroup.

Table S1. PCR-based haplotyping of DNA extracts from previous study.

Table S2. Archeological context and isotopes.

Table S3. Shotgun sequencing output and mapping data.

Table S4. mtDNA capture sequencing output data and mapping.

Table S5. 1240K sequencing output data and mapping.

Table S6. Schmutzi estimation of mtDNA contamination.

Table S7. ANGSD X chromosome contamination estimate on 1240K libraries.

Table S8. Haplogroups and private mutations for each mtDNA capture (phylotree 17).

Table S9. Complete list of NRY haplogroups with identifying ISOGG markers for 1240K capture sequences.

Table S10. Sex estimates from shotgun and genome-wide capture data.

Table S11. Sex estimates from shotgun data based on Rx values.

Table S12. Admixture CV error values for each component and individual.

Table S13. Shotgun reads with PMDtools threshold 3 filtered and skoglund sex estimate of filtered reads.

Table S14. Haplogroup calling of selected individuals before and after PMD (threshold 3) filtering.

Table S15. READ pairwise kinship-based estimate.

Table S16. Pairwise estimate of kinship and coefficient of relatedness.

References (52–58)

Supplementary Materials and methods

1. Historical background of Alemanni and Niederstotzingen

Germanic groups started to form permanent settlements in the Limes-Hinterland in the late 3rd and early 4th century AD. These groups purportedly originated from Elbgermanic region between the Baltic Sea and Thüringen forest to form the Alemannen tribe (circa 300 AD) under Roman patronage. From 350 AD the Alemanni began to rebel against Roman military rule and the power of warlords grew. Between 360 and 430 AD settled lifestyle and mobile war parties co-existed across Alemannia (1).

In the middle of the 5th century AD clear changes in the burial practices and artefacts are observed in the Alemannic archaeological record. These changes possibly reflected several independent migration waves and different political and military strategy. The Alemanni abandon old traditions and integrate new trades. From *circa* 480 AD burials are West-East orientated (previously North-South) and multiple burials appear, indicating proselytization (4). Horses are buried in the same graveyards as humans and precious artefacts are buried along with individuals that bare resemblance to artefacts from Northern Bohemia, Vinarici and the Middle Danube region (Moravia, Slovakia, and Northern Hungary). Artefacts typical of the Mediterranean and Near East indicate contacts of the Alemanni with the Byzantines. This supports the notion of migration and integration of new foreign groups.

These migrations began around 451/455 AD after the death of Attila (2). The power of the Huns decreased in the Danube region and Germanic tribes migrated away. Compact political structures were formed by increasingly centralized settlements, where political elites lived, resulting in closer social connections between heterogeneous Alemanni. Rank in this society was based on the size of one's retinue (*Personenverbandstaat*) and possession of valuable materials rather than fixed territorial control (4). Transition of power was not based on inheritance either, but could be passed between high-ranking individuals in a group. This is reflected in the archaeological record of Alemanni and other Germanic Migration-period groups by the observation of burials with combinations of family and unrelated people living together in so-called familia (30).

Clovis I defeated the Alemanni in 497 AD and established Alemannia as an administrative area under the overlordship of the Merovingian Kingdom and Frankish Dukes (4). In the following three centuries, naming of groups became more rigid, along with other Germanic groups including Thuringians, Bavarians and Burgundians (3). This brought to an end the Germanic migrations in the Migration-period. In the following three centuries the Merovingians subjected Alemannia to political, economic and social changes, including Christianisation. Around 600 AD powerful families differentiated and became nobles. These nobles bestowed artefacts and territory to individuals that were indicative of rank and purpose and were subsequently buried with those people.

2. Historical designations

Tacitus first described the Suebi in the 1st century AD as a homogenous confederation of barbarians across Western Germany. Cassius Dio first documented the Alemanni in 213 AD along

the Limes frontier in the Upper Rhine region (1, 2). These names were probably designations by Romans to classify an array of heterogeneous Germanic groups at the frontiers of the Empire. Accounts of Suebi and Alemanni differ throughout the centuries, some accounts designate them as distinct whereas others use the terms interchangeably. Alemanni have periods of stark geographic discontinuity in historical accounts. For example, in the early 4th century AD they disappear from records after losing conflicts against the Romans only to reappear decades later. In the mid-4th century AD, Armanius divides the Alemanni into Bucinobantes and Lentienses. But these appear to be geographic rather than ethnic distinctions (1, 2).

Interchangeability of names with other Germanic groups is common in the historical accounts. Gregory of Tours mid-6th century historian writes that Suebi and Alemanni are one people. Yet earlier accounts distinguished the two. The Suebi came to the Upper Rhine around 400 AD, and a union of the two groups may have occurred between 454 and 474 AD. The union of Suebi and Alemanni into Alemanni may have been against the Romans or rival Germanic groups such as the Franks.

3. Archaeological context, PCR based analysis, osteological description and stable isotopes

Previous to this study, archaeologists excavated twelve graves and recovered the remains of thirteen individuals and a rich assemblage of artefacts that dated the site to the beginning of the 7th century A.D. (6, 8). These artefacts and the presence of swords buried with all adult males show evidence of a Warrior class that were in contact with Lombards, Franks and Byzantines (fig. S1 A-D). The burial is located approximately at the site of a Roman crossroads, which was still maintained at the time (Fig. 1). The rich assemblage of grave goods at the burial indicates that these individuals were associated to a military outpost guarding an important land route. Also discovered at the site were horse burials and equestrian gear, inferring that the individuals were highly mobile. Belt inscriptions and style dated the burial to *circa* 580 to 630 AD (8).

Grave 1: Lance, shield, saex, double-edged-sword.

Grave 2: Saex.

Grave 3A: Lance, shield, saex, double-edged-sword, arrows, and bridle with silver pressed sheet metal fittings of Byzantine ornamentation.

Grave 3B: Lance, shield, saex, double-edged-sword.

Grave 3C: Lance, shield handle, saex, double-edged-sword.

Grave 4: Belt, pearls and golden ring.

Grave 5: Belt ornamentation dated to beginning of 7th century

Grave 6: Double-edged-sword, belt and bridle originating from Lombard Italy. Belt ornamentation dated to beginning of 7th century.

Grave 7: Beads with no human remains. Evidence of being plundered.

Grave 8: Horse remains.

Grave 9: Lance, shield, shield handle, saex, double-edged-ring-sword. The ring-sword has a silver pommel and bead golden decorative button, and the lance engravings indicate Frankish origin.

Grave 10: Double-edged-sword.

Grave 11: Remains of two horses.

Grave 12a: Shield, shield handle, double-edged-sword, lamella armour Byzantine style.

Grave 12B: Double-edged-sword, lance, shield, lamella helmet Byzantine style.

Grave 12C: Double-edged-sword.

Previous studies PCR based studies retrieved the genetic sex for some of the individuals. Also the hypervariable region of the mitochondrial genomes were partly reconstructed which show the haplogroup for some of the individuals (table S1).

Age-at-death estimates of individuals show a combination of three children and ten adults at the site (table S2). Strontium isotope ($^{87}\text{Sr}/^{86}\text{Sr}$) and Oxygen ($\delta^{18}\text{O}$) isotope analysis (estimated in previous study) show that all individuals had local geographic origin with the exception of 3B and 10, who have 'non-local' signals (fig. S2) (8). The $\delta^{18}\text{O}$ support a childhood spent in a higher altitude region such as the Alps. Together $\delta^{13}\text{C}$ and $\delta^{18}\text{O}$ values estimate that all consumed a primarily terrestrial diet and thus do not support any significant period of settlement close to the sea.

4. Next generation sequencing and analysis

Preparation of DNA and sequencing

Teeth were sampled from each individual and dentine was separated. This was sterilized with bleach solution and UV-light in a clean room at the EURAC Institute for Mummies and the Iceman Bolzano, Italy. Silica based extraction was used to extract DNA from ~250mg of milled dentine (31). Double-stranded Illumina libraries were prepared using the protocol for ancient DNA (aDNA) and double indexed (32, 33). DNA extracts were sent to the aDNA facility at the University of Tübingen, Germany for library preparation, and subsequent shotgun sequencing and mitochondrial DNA (mtDNA) probe capture (52). Prior to nuclear SNP capture (1240K) (24), library preparation incorporated half-UDG (Uracil-DNA Glycosylase) treatment of extracts to reduce lesions to DNA caused by time dependent deamination of aDNA (34). Where there were multiple genomic libraries from the same individual, the library with the highest percentage of endogenous DNA was chosen for nuclear capture (table S3). Half-UDG libraries were transferred to the Institute for Human History at the Max Planck, Jena, Germany for 1240K capture and sequencing. 1240K capture enriched libraries for 1.24 million SNPs.

Shotgun and mtDNA capture libraries were sequenced on an Illumina HiSeq 2500 (75bp paired-end sequencing kits). The 1240K captured libraries were multiplexed and sequenced on an Illumina HiSeq 4000 and NextSeq (75bp paired-end sequencing kits).

Raw data processing and quality control

Raw paired end data processing and quality control followed the pipeline of EAGER (37). Clip&Merge had a minimal fragment length of 30bp after trimming removed 2bp from 5' and 3' termini to reduce residual deamination. BWA seeding was disabled (-l 1000) for greater inclusion of deaminated sequences (53). Reads were mapped to the human genome (Build Hg19) (39) for shotgun and autosomal capture. The mtDNA capture was mapped to the mt reference (rCRS) (40). Samtools mpileup (54) with Pileupcaller (<https://github.com/stschiff/sequenceTools/tree/master/src-pileupCaller>) were used to genotype mapped reads to EIGENSTRAT format. For all downstream analyses, the mapping quality and base quality threshold for downstream analysis were > 30. Summary of EAGER outputs show that shotgun data have considerable variety of reads mapping to the target loci from less than 1% to over 75% endogenous content (table S3). This indicates that DNA preservation is considerably varied between the individuals and even in the samples taken from the same individual. The EAGER output of the mtDNA and 1240K capture show enrichment of percentage reads mapping to target loci (table S4 and S5). For 1240K capture, individuals 1, 3A,

3B, 3C, 6, 9, 12B and 12C had sufficient enrichment for downstream population genetics analysis. PMDtools was applied to mtDNA capture and shotgun data (non-UDG treated) to filter potential modern contamination and serve as another level of authentication (22) (table S13 and S14).

Contamination estimates and authentication

mtDNA contamination was analysed using Schmutzi (42), to estimate the level of contaminating reads in the mtDNA captured sequenced libraries. The data show that mtDNA capture contamination was low except for individuals 2, 10 and 12a having contamination above 5% (table S6).

ANGSD (43) estimated the autosomal contamination based on mismatches in males at the X-chromosome in 1240K libraries. The data show individuals with sufficient X-chromosome coverage have low contamination in the nuclear DNA (table S7).

The presence of deamination lesions at 5' and 3' ends in non-UDG treated libraries (shotgun and mtDNA capture) was quantified with MapDamage (41) to provide further evidence of the presence of endogenous aDNA. The average deamination rate is 12% at 5' termini for shotgun libraries; two libraries show low deamination at or below 5% (2, 5 and 12b) suggesting presence of modern contamination. However, mtDNA capture has an average deamination of 22% at 5' termini, for individuals 2 and 12b deamination rates increase above 25% post-enrichment, suggesting that ancient sequences are also present in rates that are appreciable enough to be effectively filtered (fig. S3). PMDtools (threshold 3) filtration of contaminated mtDNA captured libraries showed that 2 and 5 had consistent haplogroups, while 12A was less derived owing to reduced coverage (table S14).

Uniparental markers and sex estimation

Consensus mitogenome sequences were created with log2fasta (quality > 20) (42). IGVtools was used to visualise bam files and validate haplotypes at contaminated or low coverage loci (19). The haplotypes and haplogroups of the mitogenomes were identified using Haplofind and phylotree17 (table S8) (44, 45).

NRY genotypes were stringently called with ANGSD to avoid potential erroneous calling due to miscoding or low coverage. C->T and G->A transitions with <2X coverage were disqualified due to potential sequence error or residual deamination lesions. The NRY haplotypes were identified by calling genotypes that overlapped with the 1240K array and the ISOGG database 11.349 (<http://www.isogg.org/tree>). Haplotyping was assisted with yhaplo tool (55) (table S9). The partial haplogroups of ten individuals are called from the 1240K. Individuals 10 and 12a had insufficient coverage for popgen analysis but had enough to identify NRY haplotypes of the R1 lineage. Individuals 1, 3A and 9 have matching haplogroups, but at their most derived loci have different haplotypes. This does not exclude paternal relation, as R1 SNPs are consistent across the same ancestral tree and incomplete coverage on the Y-chromosome tree is observed for NRY haplotypes for the entire cohort.

To identify the genetic sex, shotgun data were analysed with a python script for genetic based estimates of sex chromosome reads X and Y (47). The normalised proportion of X chromosome reads to autosomal reads was used to help estimate sex in extremely low covered shotgun

libraries (23) (table S11). Sex estimates were also made from autosomal captures which were based on the ratio of captured reads overlapping with 1240K autosomal SNPs to the sex chromosomes, this is a visual guide and not a statistically significant estimate of sex (table S10 and S11 and fig. S4). Shotgun data show that individuals 2, 5, 10 and 12a had statistically insignificant estimates of sex but are consistent with maleness. PMDtools threshold 3 was applied to investigate if sex estimates were consistent after filtering (table S13). The PMD filtered shotgun data has less statistical robustness, individual 2 and 5's sex cannot be estimated from PMD filtered data as they lose nearly all sex chromosomal reads. Individuals 3A, 3C and 12B filtered libraries lose statistical significance for sex estimates. All individuals have relatively high Y chromosome SNP coverage in 1240K enriched libraries, which suggests maleness (24).

Population genetics

Niederstotzingen genotype data were formatted with eigenstrat convert and merged using mergeit to modern West Eurasians and North Africans from the Human origins dataset (Fig. 2) (26, 56). The ancient individual's genotypes were called with pseudo-diploid method (11, 12, 24).

Population affinity was estimated with smartpca and admixture (56, 57). Ancient individuals were projected on modern West Eurasian data for PCA plotting. Prior to admixture analysis genotypes were pruned to reduce linkage disequilibrium (plink --indep-pairwise 200 25 0.5) (58). Each Niederstotzingen individual was separately analysed against West Eurasian and Middle Eastern/North African individuals in unsupervised admixture, this was to reduce artefacts of aDNA from potentially driving ancestral components. The K value of five was selected based on having the lowest CV error for each individual (table S12). In addition, to select K5; careful analysis of the ADMIXTURE results was required to avoid erroneous interpretation of the ancestral components or results (51). The PCA and admixture data were plotted with R package ggplot2 (59) and pophelper (60) respectively (Fig. 2 and fig. S5).

Outgroup F3-statistics for each population in the human origins dataset were used to formally estimate shared genetic drift among individuals compared to a common outgroup population (25, 26). The African Mbuti population was used as an outgroup to test against West Eurasian variety (table S5). F3-stats match the estimated ancestry for the theorised Northern/Eastern/Central European individuals mentioned above but show a cryptic genetic affinity for individuals 3B and 3C. These have the strongest relatedness to modern Northern Spanish, yet this affinity is relatively weak overall (fig. S8 and S9). This may be explained by recent admixture of 3B and 3C ancestors with south western European populations.

Kinship analysis based on genome wide analysis

Often kinship studies require an array of diploid genotype SNP likelihoods for inheritance by state (IBS) estimates (15). Since the genotypes called in this analysis are low covered (1-2X covered) and are all pseudo-diploid, IBS needed to be estimated for the homozygosity of the genotypes. Pairwise estimates of kinship to 2nd degree were made with READ (relationship estimation from aDNA) (27). READ calculation was based on normalised proportion of non-matching alleles (P0) across the 1240K in non-overlapping 1Mbps blocks (table S15). READ is adapted for pseudo-diploid genotypes from GRAB software, which is a software applied to modern whole genome sequencing data and estimates relatedness to 5th degree. READ analyses data in TPED/TFAM format, which was converted using plink. P0 values are >0.9 for unrelated individuals, between 0.9 and 0.8 for second degree individuals, between 0.8 and 0.65 for first

degree individuals, and identical twins/identical are <0.65. READ accounts for population diversity and mitigates potential ascertainment bias in the dataset.

Pairwise non-normalised estimates of P0 were also made for all overlapping non-matching alleles. From this the coefficient of relatedness was estimated for each of the pairs using the following algorithm:

$$R = 1 - ((P0 - X) / X)$$

Where X is equal to the highest P0 divided by two in the cohort (table S16).

Supplementary Figures



Fig. S1. Photographs of burial goods with most specific cultural identifying markers. (A) Grave 12 Byzantine lamella helmet and armour (reconstruction). **(B)** Grave 9: equestrian gear with Frankish ornamentation. **(C)** Grave 6: Longobard ornamented double-edged-sword and armour. **(D)** Grave 3A: Byzantine equestrian gear with silver ornamentation. Copyright: Landesmuseum Württemberg, P. Frankenstein/H. Zwietasch.

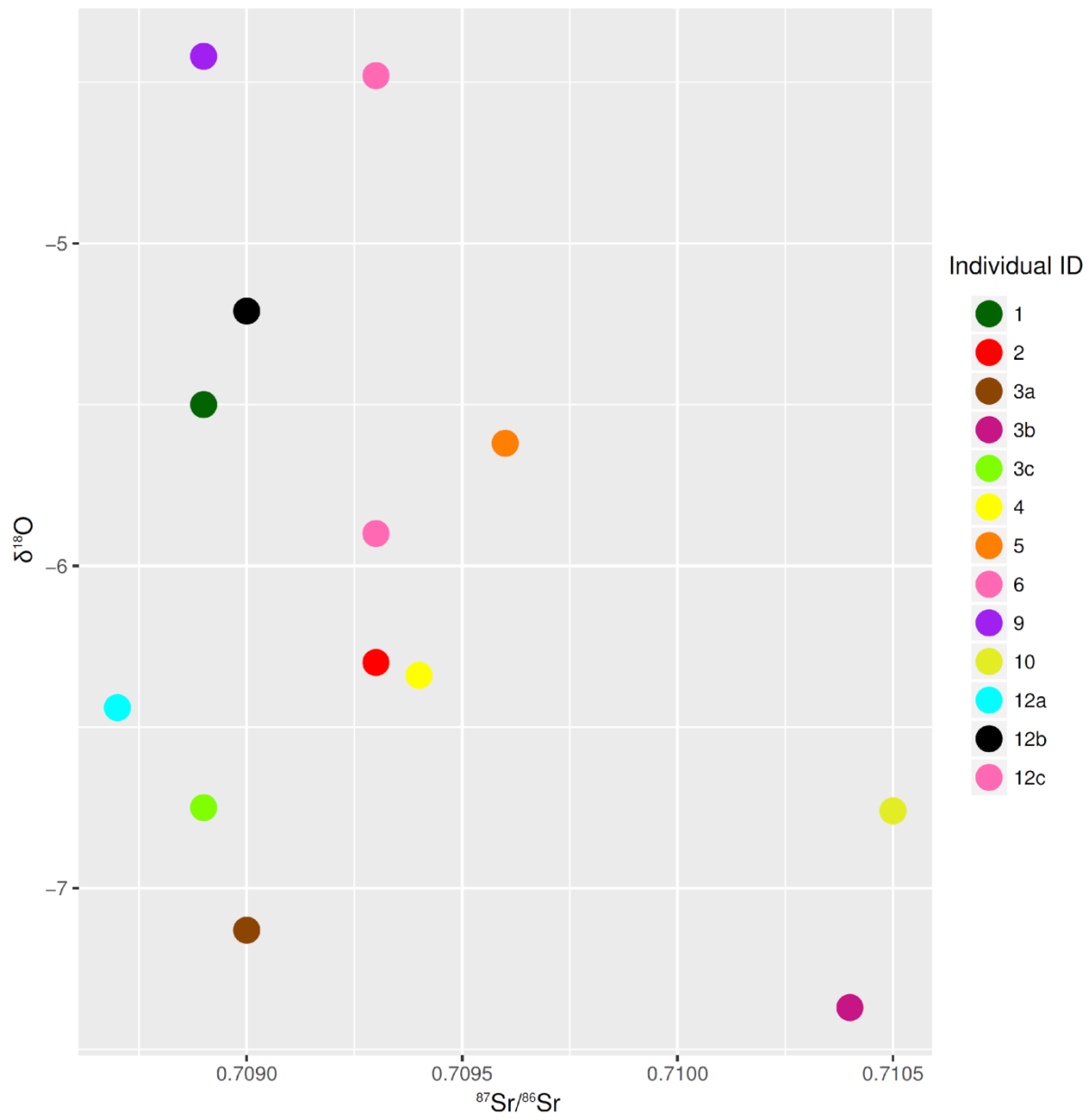


Fig. S2. Isotope $^{86}\text{Sr}/^{87}\text{Sr}$ and $\delta^{18}\text{O}$ values for enamel from teeth.

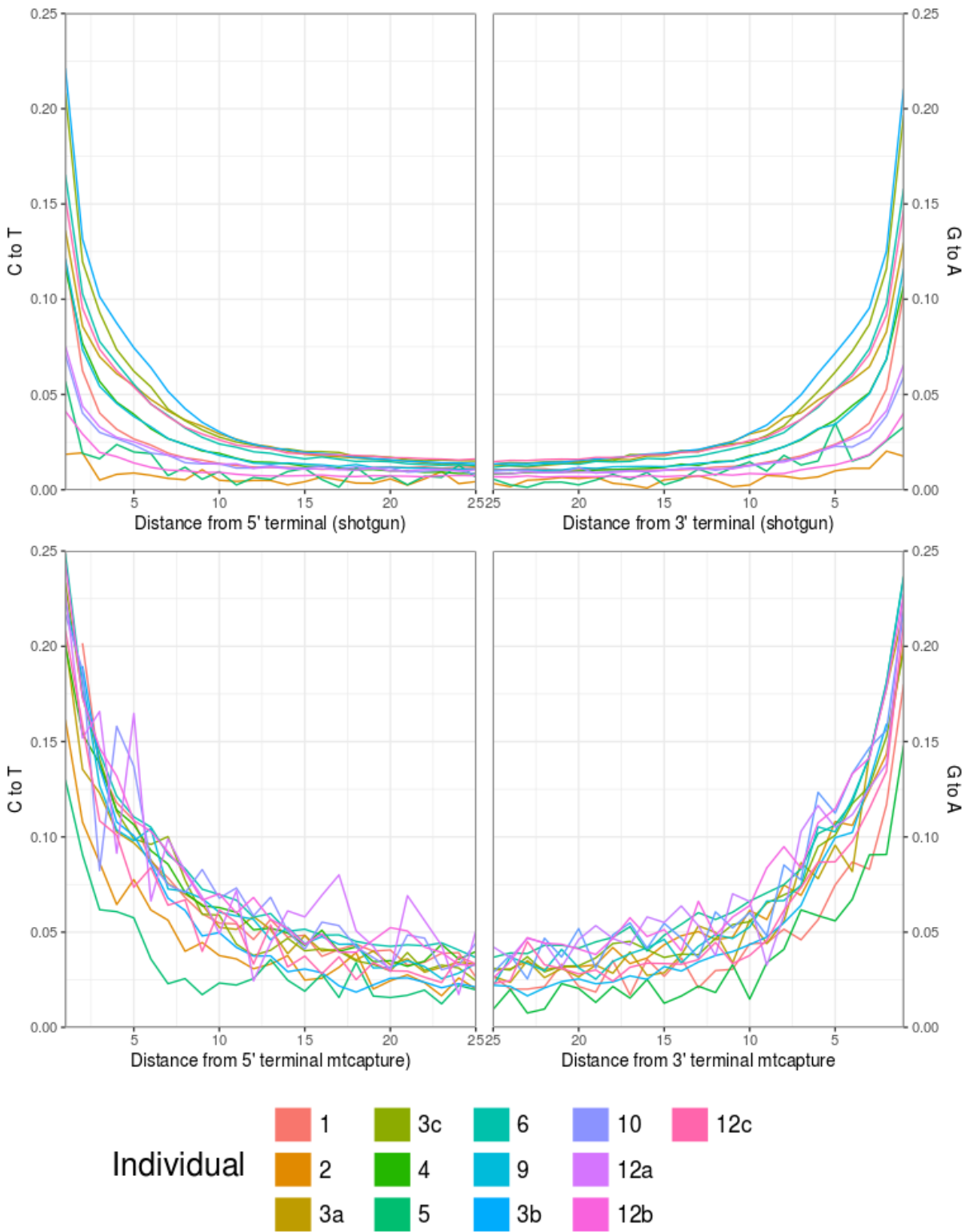


Fig. S3. Overlaying shotgun and mtDNA deamination plots from mapDamage quantification against the reference genome.

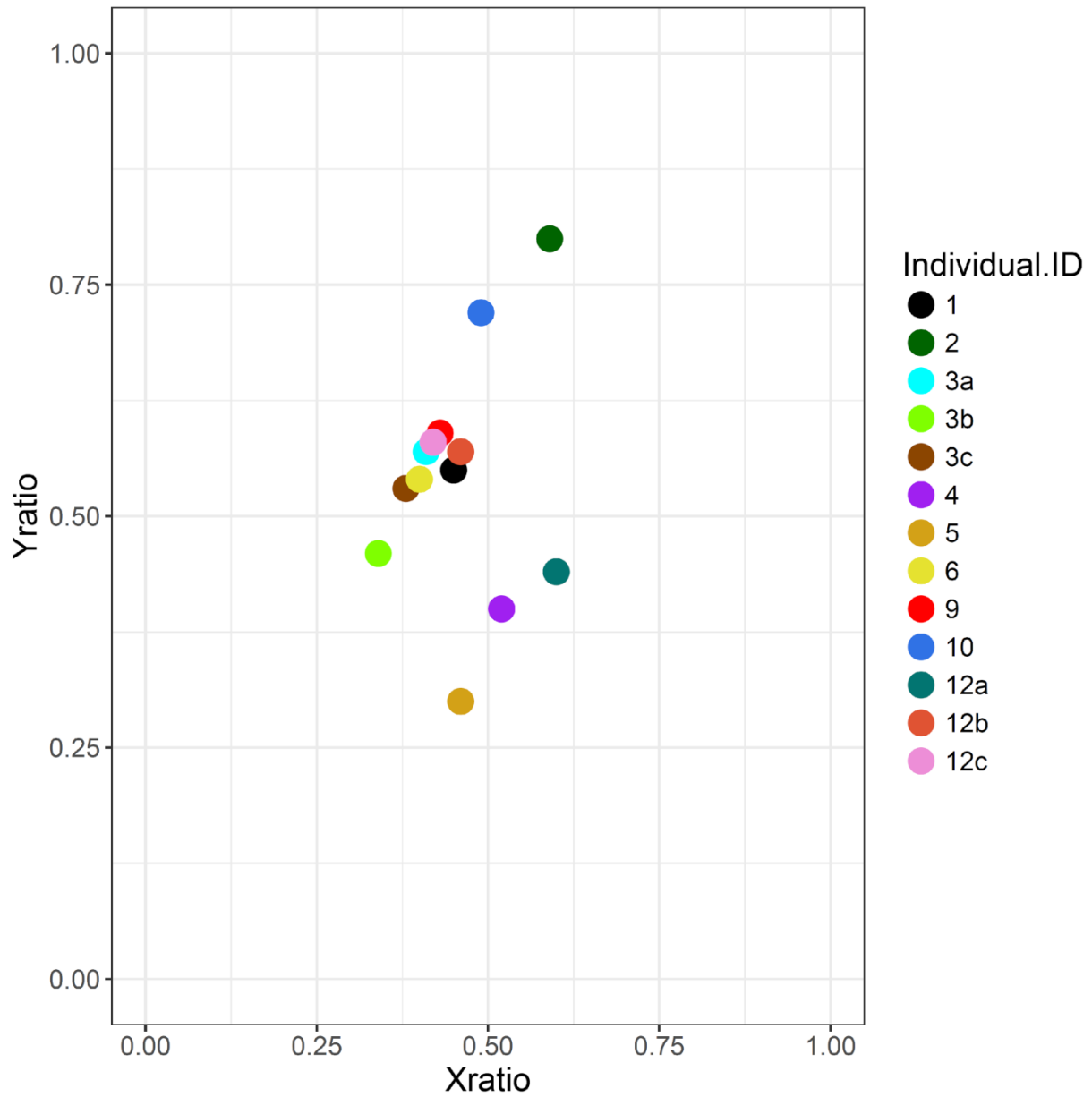


Fig. S4. Genetic sex estimates from genome-wide capture. Relative proportions of called X and Y genotypes against the autosomal genotypes. Ratio suggests that all individuals are male.

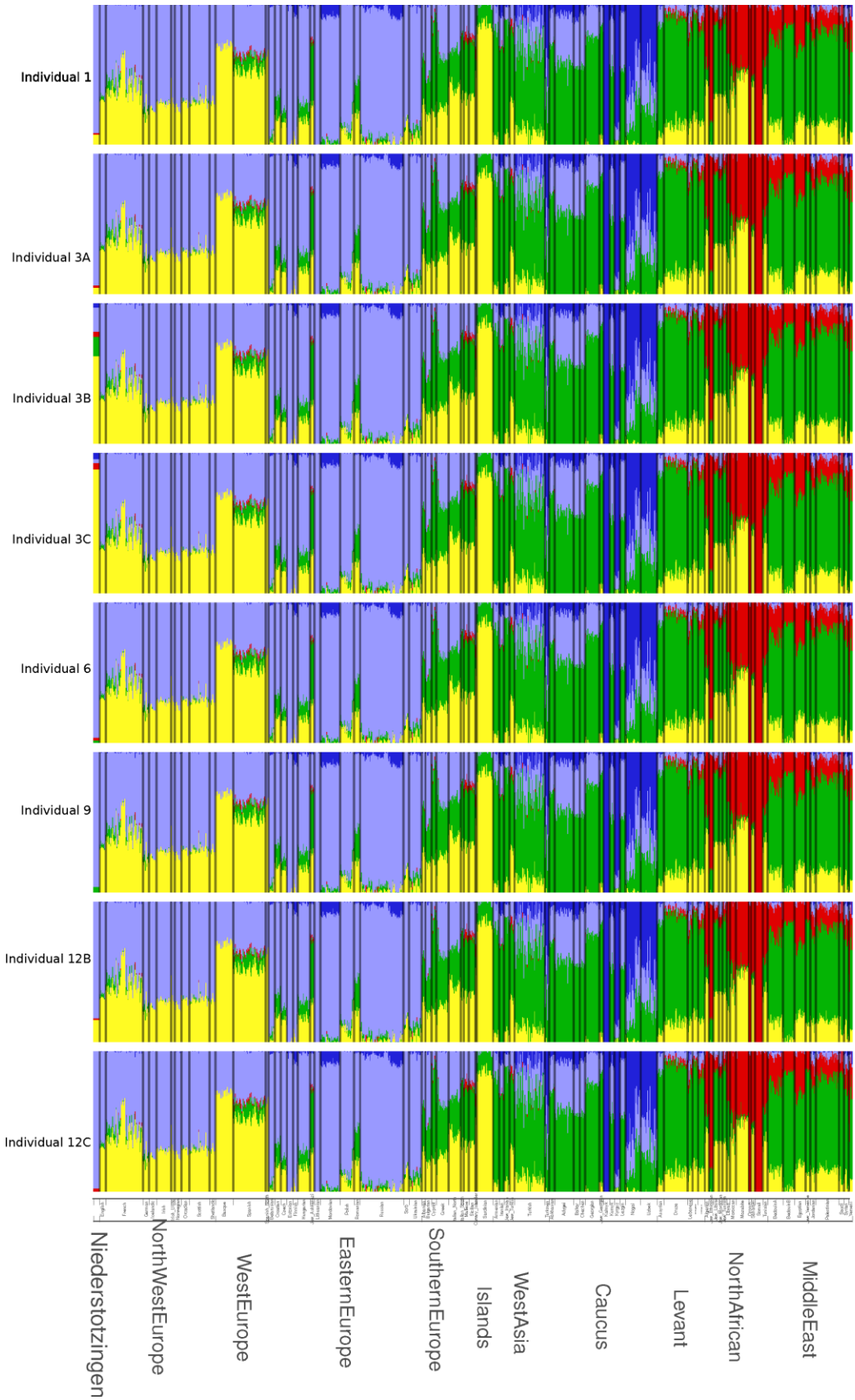


Fig. S5. Admixture estimates for west Eurasians, Niederstotzingen, and selected ancient individuals. Estimates based on five ancestral components. The ancestral components of each ancient individual are on the left hand side of the graph.

F3 (Niederstotzingen 1;X;Mbuti)

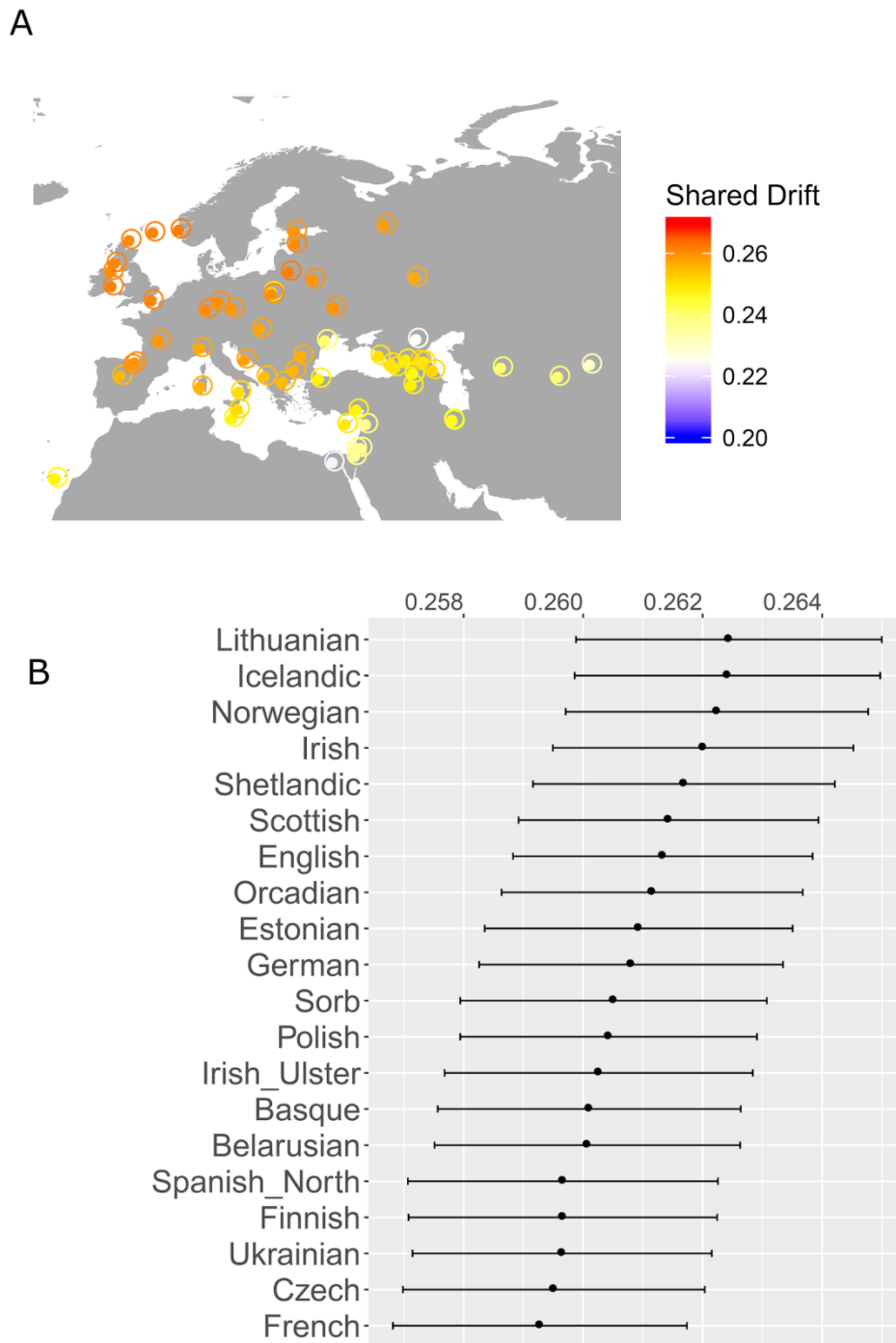
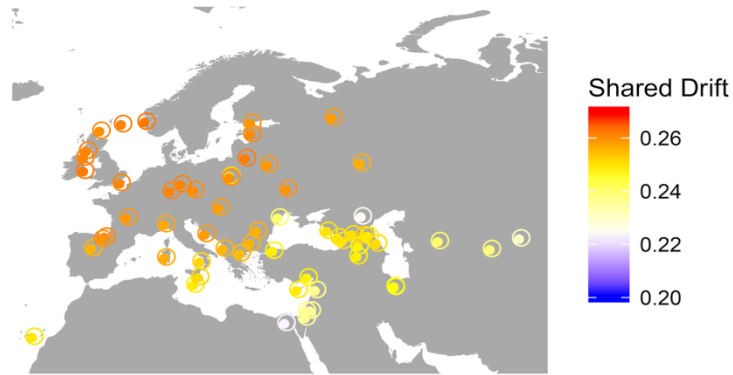


Fig. S6. F3 outgroup statistics for Niederstotzingen 1 using Mbuti as an outgroup. (A) f3 values plotted geographically across Western Eurasia. **(B)** 20 Eurasian populations with highest f3 values for each individual plotted on a line plot showing margins of error.

F3 (Niederstotzingen 3A;X;Mbuti)

A



B

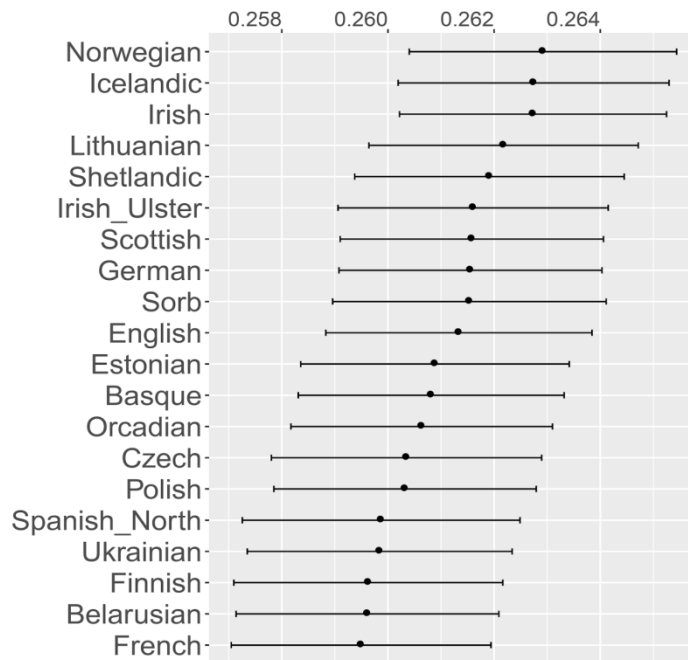


Fig. S7. F3 outgroup statistics for Niederstotzingen 3A using Mbuti as an outgroup. (A) f3 values plotted geographically across Western Eurasia. **(B)** 20 Eurasian populations with highest f3 values for each individual plotted on a line plot showing margins of error.

F3 (Niederstotzingen 3B;X;Mbuti)

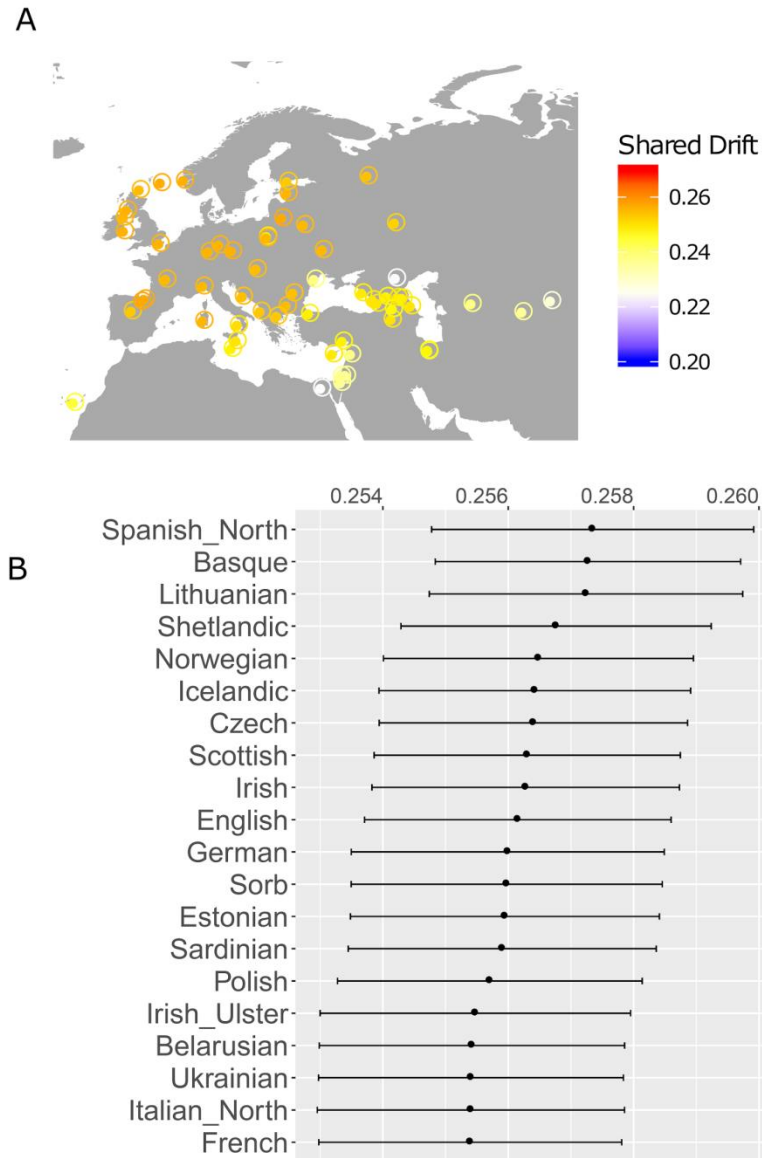
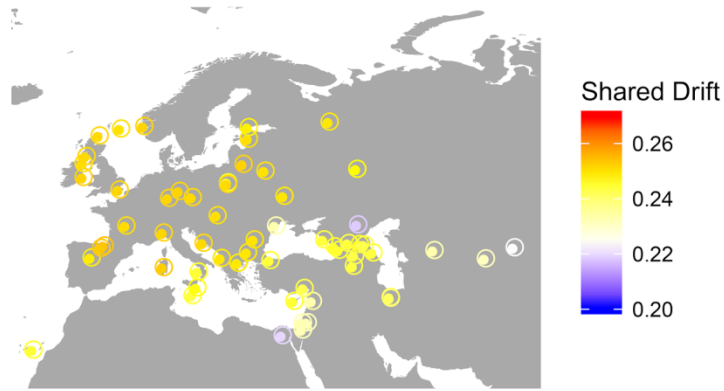


Fig. S8. F3 outgroup statistics for Niederstotzingen 3B using Mbuti as an outgroup. (A) f3 values plotted geographically across Western Eurasia. **(B)** 20 Eurasian populations with highest f3 values for each individual plotted on a line plot showing margins of error.

F3 (Niederstotzingen 3C;X;Mbuti)

A



B

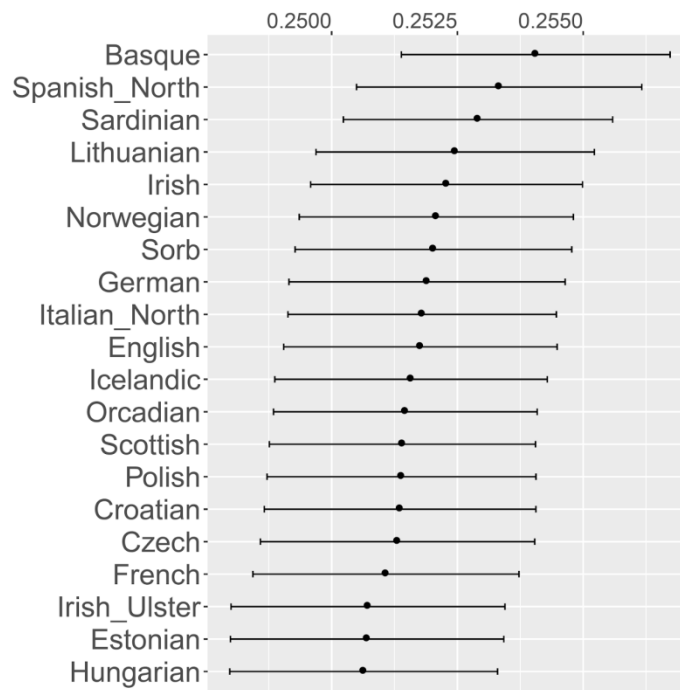


Fig. S9. F3 outgroup statistics for Niederstotzingen 3C using Mbuti as an outgroup. (A) f3 values plotted geographically across Western Eurasia. **(B)** 20 Eurasian populations with highest f3 values for each individual plotted on a line plot showing margins of error.

F3 (Niederstotzingen 6;X;Mbuti)

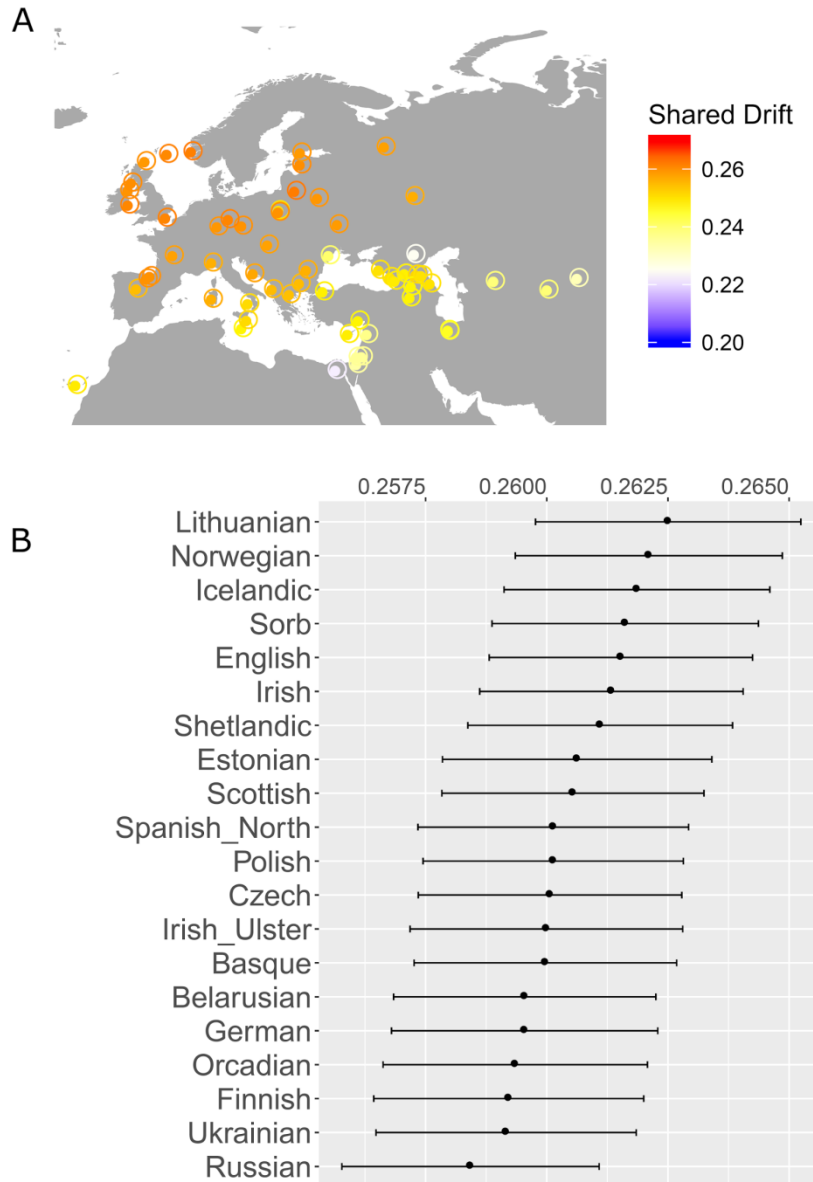
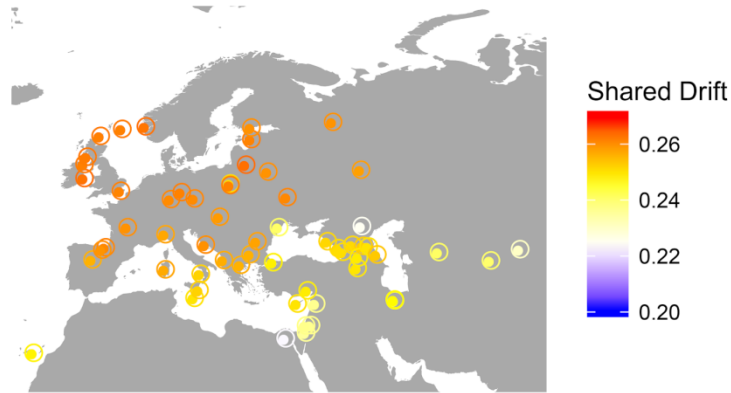


Fig. S10. F3 outgroup statistics for Niederstotzingen 6 using Mbuti as an outgroup. (A) f3 values plotted geographically across Western Eurasia. **(B)** 20 Eurasian populations with highest f3 values for each individual plotted on a line plot showing margins of error.

F3 (Niederstotzingen 9;X;Mbuti)

A



B

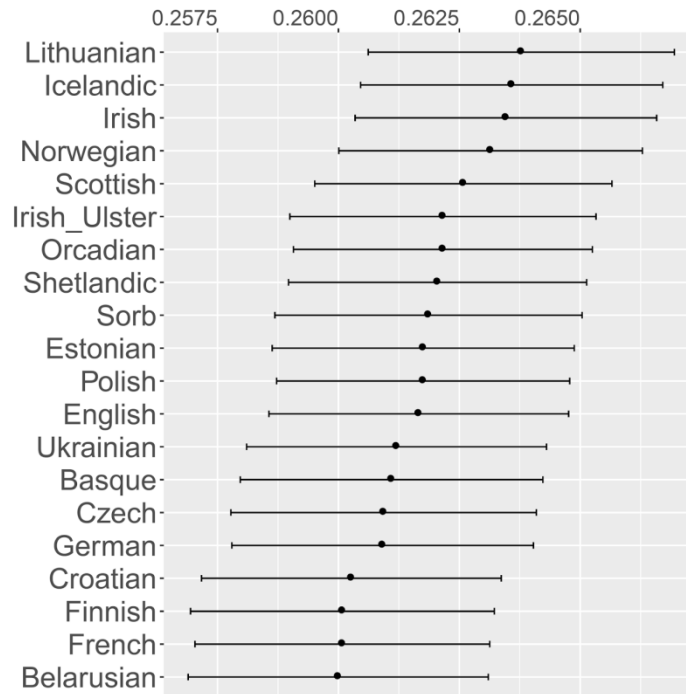
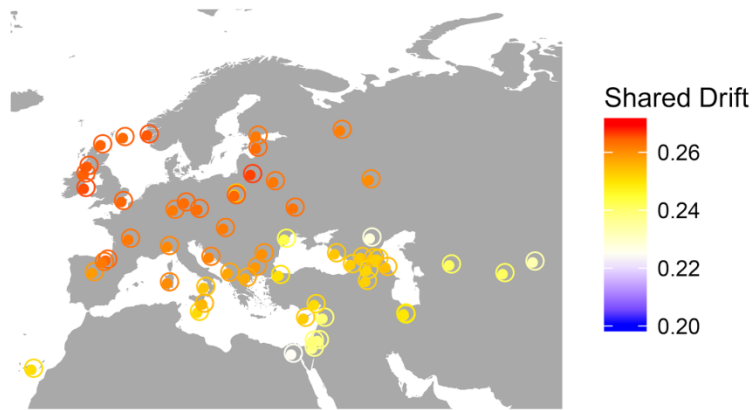


Fig. S11. F3 outgroup statistics for Niederstotzingen 9 using Mbuti as an outgroup. (A) f3 values plotted geographically across Western Eurasia. **(B)** 20 Eurasian populations with highest f3 values for each individual plotted on a line plot showing margins of error.

F3 (Niederstotzingen 12B;X;Mbuti)

A



B

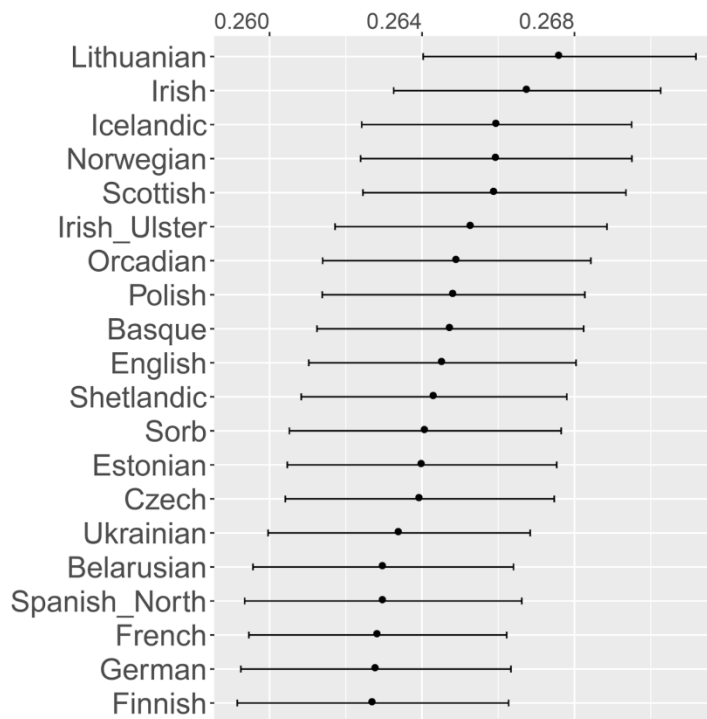


Fig. S12. F3 outgroup statistics for Niederstotzingen 12B using Mbuti as an outgroup. (A) f3 values plotted geographically across Western Eurasia. **(B)** 20 Eurasian populations with highest f3 values for each individual plotted on a line plot showing margins of error.

F3 (Niederstotzingen 12C;X;Mbuti)

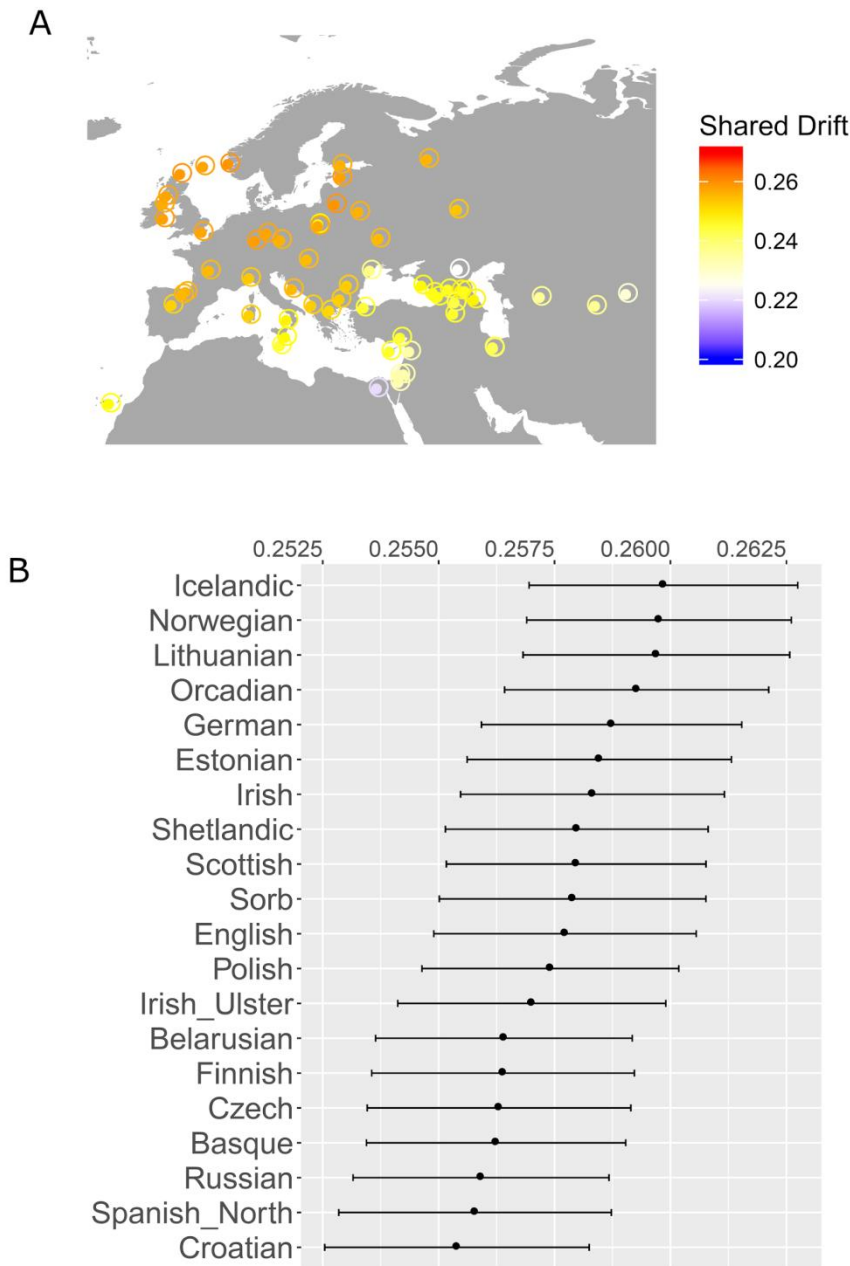


Fig. S13. F3 outgroup statistics for Niederstotzingen 12C using Mbuti as an outgroup. (A) f3 values plotted geographically across Western Eurasia. **(B)** 20 Eurasian populations with highest f3 values for each individual plotted on a line plot showing margins of error.

Supplementary Tables

Table S1. PCR-based haplotyping of DNA extracts from previous study. Coloured rows indicate multiple burials. *Anthropological Sex estimates from Creel 1967/Wahl 2011.

Individual ID	Extraction ID	Sample	Sex estimate*	mtDNA haplogroup	Single Nucleotide Polymorphisms (SNPs)
1	1326	Tooth 44	m/m	K	T16093C, T16224C, T16311C
2	1327	Tooth 42	-/-	H	G16129A, A16316G
3a	1328	Tooth 44	m/m	K	T16093C?, T16224C, T16311C
3a	1572	Tooth 42		K	T16093C, T16224C, T16311C
3b	1329	Tooth 44	m/m	I5a	G16129A, C16148T, C16223T, G16391A
3b	1573	Tooth 12		I5a	G16129A, C16148T, C16223T, G16391A
3c	1330	Tooth 15	m/m	T	T16126C, C16294T
3c	1574	Tooth 44		T	T16126C, C16294T
4	1331	Tooth 33	-/-	K	T16093C, T16224C, T16311C
5	1332	Tooth 61	-/-	K	T16093C, T16224C, T16311C
6	1333	Tooth 36	?/m	-	CRS
9	1334	Tooth 23	m/m	X	T16189C, C16223T, C16278T
10	1335	Tooth 45	m/-	-	T16189Y, T16224C, T16356Y
10	1575	Tooth 34		-	T16189Y, T16224C, T16356Y
12a	1336	Tooth 34	m/m	R	T16093C?, C16221T
12a	1576	Tooth 35		R	T16093C, C16221T
12b	1337	Tooth 44	m/m	X	T16189C, C16223T, C16278T
12b	1577	Tooth 32		X	T16189C, C16223T?, C16278T
12c	1338	Tooth 34	m+w/m	U5a	C16256T, C16270T, A16399G
12c	1578	Tooth 45		U5a	C16256T, C16270T, A16399G?

Table S2. Archeological context and isotopes. *Strontium values support non-local provenance (data from previous study). Coloured rows indicate multiple burials. §Wahl 2011.

Individual ID	Age estimate (years)§	Sex estimate (osteological)	$^{87}\text{Sr}/^{86}\text{Sr}$	$\delta^{13}\text{C}$	$\delta^{18}\text{O}$	Archeological context
1	40-50	male	0.7089	-12.88	-5.5	
2	9-11	Uncertain	0.7093	-12.85	-6.3	
3a	20-30	male	0.709	-13.43	-7.13	Byzantine
3b	50-60	male	0.7104*	-13.16	-7.37	
3c	20-30	male	0.7089	-13.45	-6.75	
4	2	Uncertain	0.7094	-12.64	-6.34	
5	0.5-2	Uncertain	0.7096	-12.78	-5.62	
6	14-17	Uncertain	0.7093	-14.01	-4.48	Lombard
7	NA	NA	NA	NA	NA	
8	NA	NA	NA	NA	NA	
9	40-50	male	0.7089	-13.63	-4.42	Franconian
10	20-25	male	0.7105*	-11.21	-6.76	
11	NA	NA	NA	NA	NA	
12a	25-35	male	0.7087	-13.33	-6.44	
12b	30-40	male	0.709	-13.92	-5.21	Byzantine
12c	20-30	Uncertain	0.7093	-13.43	-5.9	

Table S3. Shotgun sequencing output and mapping data. *endogenous percentage represents all reads that map to human genome (hg19) that have mapping quality above 30 and duplicates retained. §Libraries selected for genome wide capture due to higher coverage than other subsample from the same individual. **Green** and **red** colouration represents individuals buried in multiple burials 12 and 3, respectively.

Individual ID	Library ID	# of Merge d Reads > length 30	# mapped reads prior RMDup and quality > 30	% Total Endogenous DNA*	#reads after deduplicated and mapping quality > 30	% mtDNA reads quality > 30	% reads overlap with 1240K quality > 30
1	1326 §	2601278	883832	33.98	732607	0.020	1.06
2	1327 §	2629465	5859	0.22	4740	0.004	0.01
3a	1328 §	2274652	217938	9.58	160264	0.020	0.23
3a	1572	189346	24345	12.86	9577	0.001	0.29
3b	1329	1465161	24711	1.69	19281	0.010	0.05
3b	1573 §	4325231	3350473	77.46	2321267	0.005	1.51
3c	1330 §	3146945	186096	5.91	129531	0.003	0.12
3c	1574	3932684	671661	17.08	408134	0.007	0.27
4	1331 §	3132678	313851	10.02	223767	0.012	0.24
5	1332 §	2731735	4145	0.15	2668	0.007	0.00
6	1333 §	2750558	251673	9.15	180766	0.021	0.20
9	1334 §	4385230	332779	7.59	227654	0.011	0.18
10	1335	5153487	6651	0.13	4860	0.001	0.00
10	1575 §	4274087	74763	1.75	54762	0.006	0.05
12a	1336 B	3411461	454974	13.34	367974	0.014	0.40
12a	1576 §	3251558	327741	10.08	166446	0.019	0.28
12b	1337	3681461	4849	0.13	2537	0.007	0.00

12b	1577 §	34458 07	320079	9.29	244114	0.021	0.29
12c	1338	49197 57	378718	7.70	282123	0.015	0.22
12c	1578 §	42490 45	891545	20.98	605680	0.005	0.39

Table S4. mtDNA capture sequencing output data and mapping. *% of mapped reads to rCRS reads that have map quality above 30 and prior to deduplication. §Efficiency capture measure is based on division of the percentage of reads in shotgun and mtDNA capture (% mtDNA reads in table S3). **Green** and **red** colouration represents individuals buried in multiple burials 12 and 3, respectively.

Individual ID	Library ID	# reads after C&M length > 30	# mapped reads prior RMDup > quality 30	%Endogenous DNA*	#Mapped Reads deduplicated and quality > 30	Mean Coverage unique reads	std. dev. Coverage	Capture enrichment efficiency§
1	1326	1268373	252928	19.94	16823	79.92	37.1	978.7
2	1327	3596840	53136	1.48	4766	25.09	12.44	346.8
3a	1328	2950924	277524	9.40	19436	103.72	42.47	462.0
3b	1573	3384347	120641	3.56	11605	40.4	25	670.3
3c	1330	1222172	45825	3.75	3529	15.13	6.15	1388.2
4	1331	6775001	214653	3.17	14747	76.62	26.85	273.4
5	1332	2649216	122411	4.62	2633	12.97	6.05	657.4
6	1333	4689859	390109	8.32	50098	278.7	90.14	400.0
9	1334	5323643	315358	5.92	6511	28.48	10.53	542.3
10	1575	817315	112591	13.78	1868	10.79	6.76	2494.9
12a	1576	1338414	313047	23.39	1386	8.01	4.97	1213.0
12b	1577	1941732	348687	17.96	7965	41.2	18.52	872.8
12c	1578	2669480	133618	5.01	4795	24.77	14.46	989.2

Table S5. 1240K sequencing output data and mapping. *non-UDG treated libraries. §Percentage of mapped reads to that overlap with 1240K with mapping quality above 30 and before deduplication. ~Capture enrichment efficiency is estimated from the division of the percentage of reads overlapping with the 1240K array in the capture libraries over the shotgun libraries before deduplication, (table S3). †Libraries that had insufficient enrichment for population genetics. **Green** and **red** colouration represents individuals buried in multiple burials 12 and 3, respectively.

Individual ID	Library ID	# reads after C&M prior mapping	# mapped reads prior RMDup that overlap with 1240K array	§Endogenous DNA (%) quality > 30	#reads duplicates removed and q> 30	Mean Coverage	std. dev. Coverage	genotype Overlap with 1240K	genotype Overlap with HO	Capture Enrichment efficiency~
1	1326	11019504	3782425	34.32	984227	0.85	1.14	583209	306662	32.7
2	1327*†	4231587	793951	18.76	18628	0.02	0.23	10031	5150	2790.2
3a	1328	17063625	4763700	27.92	793078	0.68	1.04	490654	260257	123.3
3b	1573	18357358	6141901	33.46	2121562	1.79	2.56	672872	374347	22.3
3c	1330	22522015	6121123	27.18	352083	0.29	0.69	254250	136862	232.5
4	1331†	3691000	121598	3.29	1948	0.00	0.06	1293	697	13.6
5	1332†	7055785	645416	9.15	5193	0.00	0.12	2798	1475	2191.0
6	1333	13671307	3485683	25.50	480461	0.41	0.78	341584	180449	129.2
9	1334	11904124	3356524	28.20	284475	0.24	0.63	208884	109961	154.6
10	1575*†	5292788	1136390	21.47	21057	0.02	0.21	13340	6922	441.2
12a	1576*†	5356151	1603754	29.94	78845	0.07	0.35	57517	29673	110.5
12b	1577	10415425	2805511	26.94	195274	0.17	0.56	138500	72868	92.9
12c	1578	9479208	2735735	28.86	433220	0.37	0.75	308135	162405	75.0

Table S6. Schmutzi estimation of mtDNA contamination. Green and red coloration represents individuals buried in multiple burials 12 and 3, respectively.

Individual	Library ID	Median	Lower	Upper
1	1326	0.03	0.02	0.04
2	1327	0.15	0.14	0.16
3a	1328	0.02	0.01	0.03
3b	1573	0.03	0.02	0.04
3c	1330	0.03	0.02	0.04
4	1331	0.03	0.02	0.04
5	1332	0.04	0.03	0.05
6	1333	0.02	0.02	0.02
9	1334	0.04	0.03	0.05
10	1575	0.06	0.04	0.08
12a	1576	0.09	0.07	0.11
12b	1577	0.03	0.02	0.04
12c	1578	0.03	0.02	0.04

Table S7. ANGSD X chromosome contamination estimate on 1240K libraries. Contamination estimate chosen from Method2: new llh with standard error (SE). **Green** and **red** colouration represents individuals buried in multiple burials 12 and 3, respectively.

Individual ID	Library ID	Contamination	SE
1	1326	0.001923	2.87E-03
3a	1328	0.014507	7.12E-03
3b	1573	0.000928	2.41E-03
3c	1330	0.040375	2.03E-02
6	1333	-0.00068	1.17E-03
9	1334	-0.00473	4.66E-03
12b	1577	0.012842	1.36E-02
12c	1578	0.000982	7.78E-03

Table S8. Haplogroups and private mutations for each mtDNA capture (phylotree 17). *missing because loci were quality filtered by log2fasta (quality > 20). **Green** and **red** colouration represents individuals buried in multiple burials 12 and 3, respectively.

Individual	Library ID	Haplogroup	Non haplogroup defining mutations	Missing mutations
1	1326	K1a	8955C,12063T,14602G	195T
2	1327	K1a1b2a1a	770T,11053G	114T,16093C*
3a	1328	K1a	8955C,12063T,14602G	195T
3b	1573	I5a1b		
3c	1330	T2	248G,515G	16296T
4	1331	X2b4	310C,3106A,13676G,16183C	
5	1332	K1a1b2a1a	770T,11053G	114T
6	1333	H65a		
9	1334	X2b4	310C,13676G,16183C	
10	1575	H1b	15955G,16183C	7028C
12a	1576	H10e1	5104T,7598A,14016A,14281T	2758G*,4104A*,4312C*,10398A,16230A*,16311T*
12b	1577	X2b4	310C,13676G,16183C	
12c	1578	U5a1a1		

Table S9. Complete list of NRY haplogroups with identifying ISOGG markers for 1240K capture sequences. Positions with multiple marker names indicate current overlapping nomenclature of ISOGG database (11.01).

Individual	position	haplogroup	Ancestral	Derived	Depth	Markers
1	19267344	R	C	A	2	P285
1	22750583	R1	C	A	1	M306,PF6147,S1
1	9989615	R1	A	G	1	P231
1	17782178	R1	C	G	1	P236
1	18914441	R1b1	C	T	2	L278
1	18656508	R1b1a	G	C	1	P297,PF6398
1	8070532	R1b1a2	T	A	1	PF6430
1	22739367	R1b1a2	T	C	1	M269
1	22796697	R1b1a2	T	C	1	CTS10834
1	8149348	R1b1a2	A	G	1	L265,PF6431
1	8411202	R1b1a2	A	G	2	PF6434
1	18381735	R1b1a2	A	G	2	PF6482,YSC0000203
1	21222868	R1b1a2	C	G	2	PF6497,YSC0000219
1	6912992	R1b1a2	T	G	2	CTS623
1	18167403	R1b1a2	C	T	2	CTS8728,L1063,PF6480,S13
1	17844018	R1b1a2a1a	T	C	1	L11,PF6539,S127
1	18248698	R1b1a2a1a	A	G	1	P311,PF6545,S128
1	17663668	R1b1a2a1a1c2b2b	T	A	1	Z347
1	7792995	R1b1a2a1a1c2b2b1a	T	C	1	S380,Z329
1	16601300	R1b1a2a1a1c2b2b1a1	T	A	1	S1741,Z319
1	8606022	R1b1a2a1a2c1f2a1a	A	C	1	FGC5628,Y4010
1	14316964	R1b1a2a1a2c1k	C	G	1	S730
3A	21409706	R	G	C	1	P227
3A	22750583	R1	C	A	1	M306,PF6147,S1
3A	7570822	R1	G	C	1	P294,PF6112
3A	2887824	R1b	C	A	2	PF6242,M343
3A	18656508	R1b1a	G	C	1	PF6398,P297
3A	18095336	R1b1a2	A	C	1	CTS8591
3A	22796697	R1b1a2	T	C	1	CTS10834
3A	15037433	R1b1a2	C	G	1	PF6457,CTS3575
3A	23124367	R1b1a2	G	T	1	CTS11468,FGC49
3A	10008791	R1b1a2	C	T	2	PF6274.1,S351.1,L150.1
3A	21222868	R1b1a2	C	G	3	YSC0000219,PF6497
3A	2842212	R1b1a2a	T	A	1	L49.1,S349.1
3A	18907236	R1b1a2a1a	A	C	1	PF6546,S129,P310
3A	18248698	R1b1a2a1a	A	G	1	PF6545,P311,S128
3A	17844018	R1b1a2a1a	T	C	2	PF6539,L11,S127
3A	23612197	R1b1a2a1a1c2b	G	T	1	L48,S162
3A	17663668	R1b1a2a1a1c2b2b	T	A	1	Z347
3A	22023565	R1b1a2a1a1c2b2b1a	T	G	1	Z337

3A	16601300	R1b1a2a1a1c2b2b1a1	T	A	1	Z319,S1741
3A	13487452	R1b1a2a1a2c1b1b1a3a1	T	G	1	BY451
3A	8606022	R1b1a2a1a2c1f2a1a	A	C	1	FGC5628,Y4010
3B	14469411	G	C	A	1	PF2951,L382,M3523
3B	23023554	G	C	A	1	M3618,CTS11228
3B	23793740	G	C	A	1	PF3122,M3628
3B	15204710	G	A	C	1	U21
3B	8231862	G	G	C	1	M3479,PF2877
3B	8602816	G	G	C	1	PF2890,M3487
3B	16203361	G	G	C	1	M3537,CTS5317
3B	6716150	G	T	C	1	M3448,CTS373
3B	7744050	G	T	C	1	Z3192,M3468
3B	7830068	G	T	C	1	PF2865,M3470
3B	14207268	G	T	C	1	CTS2174,M3515,PF2939
3B	17798903	G	T	C	1	M3564,CTS8023,PF3017
3B	9448354	G	A	G	1	L521,F1551,PF2899
3B	14190447	G	A	G	1	M3511,CTS2125
3B	7038432	G	C	G	1	M3454,PF2847,CTS827
3B	23343857	G	C	G	1	M3424,PF3113,CTS11907
3B	15204708	G	T	G	1	L402
3B	2785630	G	A	T	1	M3226,PF2782,CTS175
3B	8600158	G	A	T	1	M3486,PF2889
3B	18615020	G	A	T	1	M3567,PF3024,CTS9011
3B	21334507	G	G	T	1	M3582,PF3049
3B	22714204	G	G	T	1	CTS10706
3B	7930724	G	C	A	2	M3474,PF2869
3B	2681740	G	G	A	2	CTS34,M3442,PF2780
3B	2795691	G	G	A	2	CTS189,M3444
3B	7614386	G	G	A	2	PF2861,M3466
3B	14432928	G	G	A	2	PF2950,U6,P257
3B	15693336	G	G	A	2	CTS4523,M3311,PF2974
3B	21412501	G	G	A	2	M3585,PF3052
3B	17533325	G	A	C	2	PF3011,L522
3B	23151673	G	T	C	2	M3622,CTS11529
3B	14195292	G	A	G	2	PF2938,M3513,CTS2136
3B	23074190	G	A	G	2	CTS11331,M3620
3B	21162869	G	C	G	2	M3580,PF3046
3B	7309873	G	T	G	2	CTS1283,PF2855,M3461
3B	19215139	G	A	T	2	CTS10026,M3575,PF3037
3B	7927218	G	C	T	2	PF2868,M3473
3B	8563874	G	C	T	2	PF2888,M3485
3B	15397649	G	A	G	4	M3526,PF2963,CTS4101
3B	15275200	G	C	G	4	PF3134,U33
3B	19124322	G	A	T	4	PF3036,M3574,CTS9894
3B	8121059	G	G	A	5	PF2875,M3477

3B	6931141	G	C	G	14	PF2844,M3450
3B	15507383	G2	T	C	1	CTS4242,M3529,PF2967
3B	15528792	G2	T	C	1	M3530,CTS4264,PF2968
3B	15635425	G2	T	C	1	PF2971,M3531,CTS4413
3B	16903051	G2	A	T	1	PF2995,F2319,M3546,L496
3B	7571775	G2	G	T	1	PF2860,M3465
3B	17088129	G2	G	C	2	PF2999,CTS6742,M3549
3B	19119067	G2	C	T	2	PF3035,CTS9885,M3573
3B	22072097	G2	G	T	2	PF3140,P287
3B	21147058	G2	A	G	3	M3579,Z6103,Y346
3B	8545324	G2	T	A	4	M3484,F1294,PF2887
3B	21401188	G2	G	T	4	M3584,F3198
3B	23768744	G2	C	T	5	M3626,PF3120,F3536
3B	10060449	G2a	A	G	1	Z3240
3B	17571517	G2a	A	G	1	M3348,PF3013,F2529
3B	23973594	G2a	T	G	1	U5,PF3141
3B	21605685	G2a	G	C	2	PF3060,M3397
3B	17090976	G2a	C	T	2	CTS6753,PF3000,M3342
3B	8426380	G2a	T	G	3	L149.1
3B	15615340	G2a2	C	G	1	L1259,M3308,CTS4367,PF2970
3B	21151007	G2a2b	T	C	1	F3139,PF3274
3B	13671506	G2a2b	G	T	1	Z3260
3B	19461366	G2a2b	C	A	4	PF3273,M3381,CTS10449
3B	16197306	G2a2b1	A	G	1	M3319,S17953
3B	14640496	G2a2b1	G	T	1	S16240,M3295
3B	8519704	G2a2b1	G	A	2	M3268.1,PF3292.1
3B	19305343	G2a2b1	G	A	4	S22095,M3377
3C	21409706	R	G	C	1	P227
3C	21843090	R	C	G	1	P280
3C	7220727	R1b1a2	A	G	1	PF6421,YSC0000276,L773
6	7570822	R1	G	C	1	PF6112,P294
6	9170545	R1b1	C	A	1	M415,PF6251
6	17986687	R1b1a2	C	A	1	PF6475,S17,YSC0000269
6	4446430	R1b1a2	T	A	1	PF6410,M520
6	7220727	R1b1a2	A	G	1	PF6421,L773,YSC0000276
6	6912992	R1b1a2	T	G	1	CTS623
6	23124367	R1b1a2	G	T	3	CTS11468,FGC49
6	18248698	R1b1a2a1a	A	G	2	P311,PF6545,S128
6	17663668	R1b1a2a1a1c2b2b	T	A	1	Z347
9	18656508	R1b1a	G	C	1	PF6398,P297
9	7762947	R1b1a2	T	C	1	PF6425
9	8149348	R1b1a2	A	G	1	PF6431,L265
9	22190371	R1b1a2	A	G	1	PF6509
9	15037433	R1b1a2	C	G	1	PF6457,CTS3575
9	2842212	R1b1a2a	T	A	1	S349.1,L49.1

9	16601300	R1b1a2a1a1c2b2b1a1	T	A	3	Z319,S1741
9	8606022	R1b1a2a1a2c1f2a1a	A	C	1	FGC5628,Y4010
10	7570822	R1	G	C	1	PF6112,P294
12A	22750583	R1	C	A	1	S1,PF6147,M306
12A	18914441	R1b1	C	T	2	L278
12B	19267344	R	C	A	1	P285
12B	8050994	R	G	C	1	P229,PF6019
12B	21117888	R1	T	C	1	P234
12B	17782178	R1	C	G	1	P236
12B	7771131	R1	G	A	2	P238,PF6115
12B	17986687	R1b1a2	C	A	1	PF6475,YSC0000269,S17
12B	16601300	R1b1a2a1a1c2b2b1a1	T	A	1	Z319,S1741
12C	19267344	R	C	A	1	P285
12C	21843090	R	C	G	1	P280
12C	17782178	R1	C	G	2	P236
12C	18095336	R1b1a2	A	C	1	CTS8591
12C	18381735	R1b1a2	A	G	1	YSC0000203,PF6482
12C	22190371	R1b1a2	A	G	1	PF6509
12C	6912992	R1b1a2	T	G	1	CTS623
12C	28590278	R1b1a2	G	A	2	CTS12478,PF6529
12C	8149348	R1b1a2	A	G	2	PF6431,L265
12C	18907236	R1b1a2a1a	A	C	1	S129,P310,PF6546
12C	18248698	R1b1a2a1a	A	G	1	PF6545,S128,P311
12C	16601300	R1b1a2a1a1c2b2b1a1	T	A	1	Z319,S1741

Table S10. Sex estimates from shotgun and genome-wide capture data. Shotgun reads* have mapping quality above 30. †Ratio of X and Y is based on sex chromosome coverage divided by autosomal coverage on genome wide capture (fig. S4). Sex estimation of shotgun reads was also applied after PMDtools filtration (threshold 3) (table S12).

Individual ID	Library ID	# reads sex chromosomes*	# reads on Y-chromosome*	Skoglund 95% CI	Skoglund Sex Estimate	Xratio†	Yratio†
1	1326	21561	2103	0.0936-0.1015	XY	0.45	0.55
2	1327	139	11	0.0343-0.124	consistent with XY but not XX	0.59	0.8
3a	1328	4374	483	0.1011-0.1197	XY	0.41	0.57
3b	1573	56134	6221	0.1082-0.1134	XY	0.34	0.46
3c	1330	3296	349	0.0954-0.1164	XY	0.38	0.53
4	1331	5566	598	0.0993-0.1156	XY	0.52	0.4
5	1332	91	9	0.0376-0.1602	consistent with XY but not XX	0.46	0.3
6	1333	4831	501	0.0951-0.1123	XY	0.4	0.54
9	1334	6270	685	0.1015-0.117	XY	0.43	0.59
10	1575	1565	126	0.067-0.094	consistent with XY but not XX	0.49	0.72
12a	1576	5596	368	0.0593-0.0723	Not Assigned	0.6	0.44
12b	1577	7054	664	0.0873-0.1009	XY	0.46	0.57
12c	1578	17144	1836	0.1025-0.1117	XY	0.42	0.58

Table S11. Sex estimates from shotgun data based on Rx values. The estimate is based on the average normalised value of X chromosome reads to the autosomes (Rx).

Grave	Estimate	Rx	95% CI	p-value
1	XY	0.524	0.4958606- 0.5521321	8.98E-13
2	XY	0.5251 5	0.5029026- 0.5473961	1.29E-11
3a	XY	0.4597 5	0.4329936- 0.486506	1.31E-10
3b	XY	0.3915 1	0.3606837- 0.4223322	2.19E-08
3c	XY	0.4225 9	0.3966302- 0.4485537	5.81E-10
4	XY	0.4144 3	0.3837851- 0.4450749	6.22E-09
5	consistent with XY but not XX	0.6299 8	0.5888209- 0.6711337	2.18E-11
6	XY	0.4497 6	0.4244624- 0.4750625	1.22E-10
9	XY	0.4606 9	0.4379698- 0.4834112	2.02E-11
10	XY	0.5154 3	0.4849277- 0.5459297	2.77E-12
12a	consistent with XY but not XX	0.6102 1	0.5804894- 0.6399396	1.69E-13
12b	XY	0.5121 2	0.4858282- 0.5384095	1.38E-12

12c

XY

0.4512
1

0.426512-
0.475911

7.51E-11

Table S12. Admixture CV error values for each component and individual. K5 has the lowest estimated CV value for each individual analysed with West Eurasians (fig. S5).

Individual	CV error K2	CV error K3	CV error K4	CV error K5	CV error K6	CV error K7	CV error K8	CV error K9	CV error K10	CV error K11	CV error K12
Grave1	0.364	0.362	0.360	0.360	0.361	0.361	0.362	0.362	0.363	0.363	0.364
	53	32	99	89	19	78	18	48	02	67	35
Grave3 A	0.364	0.362	0.360	0.360	0.361	0.361	0.361	0.362	0.363	0.363	0.364
	44	23	91	81	11	68	97	38	01	56	31
Grave3 B	0.364	0.362	0.360	0.360	0.361	0.361	0.362	0.362	0.363	0.363	0.364
	46	25	94	83	12	7	12	43	04	55	99
Grave3 C	0.364	0.362	0.360	0.360	0.361	0.361	0.362	0.362	0.362	0.363	0.364
	41	2	89	79	1	65	09	37	87	52	21
Grave6	0.364	0.362	0.360	0.360	0.361	0.361	0.362	0.362	0.363	0.363	0.364
	45	25	92	83	12	69	1	43	07	55	28
Grave9	0.364	0.362	0.360	0.360	0.361	0.361	0.362	0.362	0.363	0.363	0.364
	45	23	92	82	12	7	13	39	02	58	22
Grave1 2B	0.364	0.362	0.360	0.360	0.361	0.361	0.362	0.362	0.363	0.363	0.364
	45	26	94	83	13	71	12	41	03	56	43
Grave1 2C	0.364	0.362	0.360	0.360	0.361	0.361	0.362	0.362	0.363	0.363	0.364
	43	23	91	81	12	68	12	39	01	48	25

Table S13. Shotgun reads with PMDtools threshold 3 filtered and skoglund sex estimate of filtered reads.

Individual ID	#reads after deduplicated and mapping quality > 30 after PMD 3 filtration	# reads sex chromosomes	# reads on Y-chromosome	95% CI	Skoglund Sex estimate
1	72215	1904	196	0.0893-0.1166	XY
2	107	3	0	0.0-0.0	consistent with XX
3a	27413	610	44	0.0516-0.0927	consistent with XY but not XX
3b	662831	14363	1373	0.0908-0.1004	XY
3c	32246	699	60	0.0651-0.1066	consistent with XY but not XX
4	32257	668	73	0.0856-0.1329	XY
5	139	1	1	NA	Not assigned
6	35690	841	81	0.0764-0.1163	XY
9	30262	751	107	0.1175-0.1675	XY
10	3976	96	7	0.0209-0.1249	consistent with XY but not XX
12a	13876	366	34	0.0632-0.1226	consistent with XY but not XX
12b	11315	305	30	0.0649-0.1318	consistent with XY but not XX
12c	117703	2904	277	0.0847-0.1061	XY

Table S14. Haplogroup calling of selected individuals before and after PMD (threshold 3) filtering. The selected individuals had Schmutzi contamination estimates above 5%.

Sequence id	Haplogroup	Haplogroup after PMD filtering
2	K1a1b2a1a	K1a1b2a1a
10	H1b	H1b
12a	H10e1	H10

Table S15. READ pairwise kinship-based estimate. The Z scores are significantly diverged from 0 to strongly support authenticity, except for pairs 1/12B and 6/9. All 1240K captured SNPs were used for kinship estimate.

Pair 1	Pair 2	Relationship	Z upper	Z lower	Normalized 2 Allele Difference	Standard Error	NonNormalized P0
1	6	First Degree	6.77	-19.36	0.761	0.006	0.195
1	3A	First Degree	10.50	-15.26	0.739	0.006	0.189
9	1	First Degree	9.76	-14.49	0.740	0.006	0.189
9	12B	First Degree	4.12	-8.82	0.752	0.012	0.193
9	3A	First Degree	9.65	-13.05	0.736	0.007	0.188
1	12B	Second Degree	1.23	-10.94	0.890	0.008	0.228
9	6	Second Degree	1.15	-10.32	0.890	0.009	0.228
3A	6	Second Degree	5.69	-9.61	0.863	0.007	0.221
3A	12B	Second Degree	2.60	-8.76	0.877	0.009	0.225
1	12C	Unrelated	NA	-16.83	1.006	0.006	0.258
1	3B	Unrelated	NA	-18.62	1.000	0.005	0.256
1	3C	Unrelated	NA	-12.47	0.980	0.006	0.251
6	12B	Unrelated	NA	-4.72	0.949	0.010	0.243
6	12C	Unrelated	NA	-15.59	1.013	0.007	0.259
6	3B	Unrelated	NA	-16.88	1.001	0.006	0.256
9	12C	Unrelated	NA	-12.24	1.009	0.009	0.258
9	3B	Unrelated	NA	-15.48	1.005	0.007	0.257
9	3C	Unrelated	NA	-9.56	0.993	0.010	0.254
12B	12C	Unrelated	NA	-10.62	1.013	0.011	0.259
3A	12C	Unrelated	NA	-16.16	1.005	0.006	0.257
3A	3B	Unrelated	NA	-17.97	1.000	0.006	0.256
3A	3C	Unrelated	NA	-4.56	0.930	0.007	0.238
3B	12B	Unrelated	NA	-14.85	1.018	0.008	0.261
3B	12C	Unrelated	NA	-17.82	1.006	0.006	0.258
3C	6	Unrelated	NA	-12.33	1.001	0.008	0.256
3C	12B	Unrelated	NA	-9.59	1.012	0.012	0.259
3C	12C	Unrelated	NA	-15.26	1.023	0.008	0.262
3C	3B	Unrelated	NA	-16.31	1.002	0.006	0.256

Table S16. Pairwise estimate of kinship and coefficient of relatedness. Estimate is based on Kennett *et al* 2017.

ID1	ID2	#SNPs overlapping	#Mismatches	Proportion of mismatches (P0)	Coefficient of relatedness	Relationship
Grave1	Grave3A	285346	54510	0.19103	0.558807997	First Degree
Grave9	Grave1	118115	22601	0.19135	0.556393814	First Degree
Grave9	Grave3A	100883	19319	0.1915	0.555262165	First Degree
Grave1	Grave6	197511	38804	0.19647	0.51776688	First Degree
Grave9	Grave12B	27938	5498	0.19679	0.515352697	First Degree
Grave3A	Grave6	174743	38926	0.22276	0.319426631	Second Degree
Grave3A	Grave12B	66876	15043	0.22494	0.302980008	Second Degree
Grave1	Grave12B	78614	17825	0.22674	0.289400226	Second Degree
Grave9	Grave6	70465	16109	0.22861	0.275292343	Second Degree
Grave3A	Grave3C	129922	31517	0.24258	0.169898152	unrelated
Grave6	Grave12B	46674	11397	0.24418	0.157827235	unrelated
Grave1	Grave3C	138996	35537	0.25567	0.071142965	unrelated
Grave9	Grave3C	50198	12917	0.25732	0.058694832	unrelated
Grave3C	Grave6	89662	23267	0.2595	0.042248208	unrelated
Grave9	Grave12C	64558	16756	0.25955	0.041870992	unrelated
Grave1	Grave12C	180095	46823	0.25999	0.03855149	unrelated
Grave3C	Grave12B	33417	8688	0.25999	0.03855149	unrelated
Grave6	Grave3B	245013	63709	0.26002	0.03832516	unrelated
Grave1	Grave3B	388706	101077	0.26003	0.038249717	unrelated
Grave3A	Grave12C	160450	41783	0.26041	0.035382874	unrelated
Grave3B	Grave12B	91422	23815	0.2605	0.034703885	unrelated
Grave9	Grave3B	138630	36117	0.26053	0.034477556	unrelated
Grave3A	Grave3B	348063	90705	0.2606	0.033949453	unrelated
Grave12B	Grave12C	42973	11206	0.26077	0.032666918	unrelated
Grave3C	Grave3B	182862	47938	0.26215	0.022255753	unrelated
Grave3B	Grave12C	225813	59320	0.2627	0.018106375	unrelated
Grave6	Grave12C	113175	29785	0.26318	0.0144851	unrelated
Grave3C	Grave12C	82593	21896	0.26511	-7.54432E-05	unrelated